

TIME SERIES ANALYSIS IN FLIGHT FLUTTER

TESTING AT THE AIR FORCE FLIGHT

TEST CENTER: CONCEPTS AND RESULTS

Russell W. Lenz
Air Force Flight Test Center

and

Bruce McKeever
Time/Data Corporation

SUMMARY

Concepts of using digital time series analysis for flight flutter testing at the Air Force Flight Test Center (AFFTC) are discussed. The AFFTC Flight Flutter Facility is described. Use of a minicomputer-based time series analyzer and a modal analysis software package is described, as are the results of several evaluations of the software package. The reasons for employing a minimum phase concept in analyzing response only signals are discussed. The use of a Laplace algorithm is shown to be effective for the modal analysis of time histories in flutter testing. Sample results from models and flight tests are provided. The limitations inherent in time series analysis methods are discussed, and the need for effective noise reduction techniques is noted. The use of digital time series analysis techniques in flutter testing is shown to be fast, accurate, and cost effective at AFFTC.

INTRODUCTION

A basic mission of the Air Force Flight Test Center (AFFTC) is the flight testing of new or modified aircraft. The testing of these aircraft and their external store configurations has produced the need for a support capability in the area of flight flutter clearance. Because of the nature of the AFFTC mission, the flutter testing method must meet the following requirements and be effective under the following circumstances:

(1) The analysis capability must be usable during the testing of all types of aircraft, and it must be general enough to cover contractor testing requirements.

(2) The test engineer may not have complete knowledge of the expected flutter characteristics. Flutter prediction analyses,

wind tunnel testing, or ground vibration testing may not have been accomplished on the configuration under test.

(3) Onboard excitation systems may or may not be installed. The input forcing function might not be measurable.

(4) An entire flutter program could consist of a single flight, limiting the time available for in-flight experiments with analysis techniques.

(5) The use of both traditional and newly developed techniques must be possible.

(6) The analysis capability must minimize program cost and flight test time yet insure flight safety.

Flutter test engineers have been analyzing time histories of data for many years by using analog techniques during postflight analysis sessions. In-flight analysis was often limited to strip chart recorder observations. Often the aircraft was equipped with an excitation system, and frequency sweeps were conducted to identify modal frequencies. The sweeps were followed by multiple frequency dwell/quick stop points to obtain damping. This method was often time consuming. If pilot-induced control surface impulses were used, it was not uncommon for the engineer to observe a record in which closely spaced modes made it impossible to determine the modal characteristics of the single modes in real time.

The potential for a nearly real-time analysis capability resulted from the development of the fast Fourier transform (FFT) in 1965. Spectral analyzers which used minicomputer technology to perform FFT's became available shortly thereafter, and the first commercial modal analysis package designed for a minicomputer analyzer was developed in the early 1970's. For the first time, flight test engineers had access to an inexpensive dedicated system which could be used to make accurate real-time modal analyses.

In 1972, AFFTC acquired, and has subsequently developed, an analysis system which meets the requirements mentioned above. The AFFTC flutter test capability was originally developed by two AFFTC structural dynamicists, Captain James A. Long, Jr., and Sergeant Robert L. Berry, and their contributions are gratefully acknowledged. A minicomputer-based time series analyzer and the associated modal analysis software are the heart of the system, which is used to apply digital time series analysis techniques to structural response data. This paper briefly describes the AFFTC Flight Flutter Facility, presents some mathematical background for the analysis techniques being used, gives examples of data obtained

during 3 years of evaluating these methods, and discusses the advantages and limitations of these nearly real-time analysis techniques.

SYMBOLS

A	amplitude of the complex frequency response function
a =	$\omega\zeta$, per sec
b =	$\omega\sqrt{1 - \zeta^2}$, per sec
C	autocorrelation, V^2
\dot{C}	derivative of the autocorrelation with respect to time
c	constant
f	frequency, Hz
g	structural damping
H	complex frequency response function
h	impulse response function, V
j =	$\sqrt{-1}$
k	resolution element number
m	mass, kg (slugs)
P	real component of the frequency response function
Q	imaginary component of the frequency response function
R	magnitude of the residue, V
r	complex residue
S	power spectrum, V^2
s	Laplace variable
T	arbitrary time in a sample data frame, sec
t	time, sec

u	dummy variable
X	Fourier transform of input signal
x	input signal, V
Y	Fourier transform of response
Y'	minimum phase power spectrum, V^2
α	attenuation or absolute damping, per sec
Δf	frequency resolution, Hz
Δt	time in data frame prior to taking an FFT, sec
ζ	viscous damping ratio
θ	phase of the residue, deg
σ	absolute damping, $2\pi\alpha$, per sec
τ	autocorrelation time lag, sec
ϕ	phase of the impulse response, rad
ω	frequency, rad/sec
*	complex conjugate

Subscripts:

i	index
x	input
y	response

FLIGHT FLUTTER FACILITY

The AFFTC Flight Flutter Facility was designed to permit test engineers to use traditional strip chart analysis techniques in conjunction with advanced digital time series analysis methods. Pulse code modulation (PCM) or frequency modulation (FM/FM) flight data are converted to analog signals which can be analyzed by either technique (fig. 1). The analog filters improve the strip chart analyses by reducing noise and isolating modes. They also prevent aliasing (frequency foldback) in the digital analyses.

The hardware and software of the AFFTC system were updated several times to meet changing requirements and to increase analysis speed. The current system configuration (fig. 2) uses a 28,000-word minicomputer. The panel control unit is used during the operation of the two-channel spectrum analyzer and the small cathode ray tube (CRT) display unit. The X-Y plotter is used to produce copies of the unit's displays. A paper tape reader/punch device is used to input or save system software. The alphanumeric/graphics display terminal is the primary input/output device. It is operated in conjunction with a hard copy unit which generates a reproducible copy in 9 seconds. A multiplexer permits the simultaneous sampling of up to 16 channels of data. Antialiasing filters (low pass filters set at 30 hertz or 60 hertz) prevent higher frequencies from aliasing or folding back to lower frequencies during the digital analysis. The sampled digital time histories and the analyzer setup information are stored on two 1.2-million-word disk units. One disk unit permits the time history data used in the nearly real-time analysis of selected data channels to be stored prior to analysis. Multiple analysis approaches may be applied to the stored data. The data disk also enables an engineer to recall additional channels of data while the aircraft is turning or refueling or when strip charts indicate that a particular channel is of interest. The second disk unit is reserved for storing the program software. The six tunable bandpass (12 low pass or high pass) filters improve strip chart analyses, permit more flexibility in the selection of antialiasing filter cutoffs, and allow bandpass-filtered signals to be analyzed digitally without having to use digital filters. A patch panel links the various system components. Not shown in the photograph are the three strip chart recorders and a programmable calculator with its associated terminal.

A reduced system can and has been used at AFFTC during flutter testing. The panel-operated, two-channel spectrum analyzer can be used in conjunction with strip chart analyses, but this approach requires more flight time and results in less overall accuracy than can be obtained by using the entire capability. The current AFFTC configuration is considered to be a minimum facility for efficient operation.

The primary mode of system operation uses the alphanumeric/graphics display terminal and selected AFFTC- or contractor-written software. The engineer uses one or more of the available analysis techniques (described later in the paper) to generate trends of modal frequency, damping, or amplitude. During AFFTC tests in which control surface impulse excitation is used, at least two response channels are analyzed before the pilot is cleared for the next test condition. For test planning purposes, approximately 4 minutes are allowed per test point, although this estimate increases if the aircraft is to be power limited during

the test. The use of the multiple analysis techniques available in the system permits the AFFTC engineers or contractors to adapt quickly to the characteristics of a particular aircraft or to changing flight conditions.

TIME SERIES/LAPLACE ANALYSIS

The digital time series analysis techniques used at AFFTC utilize the FFT to linearly transform a structural response time history into a complex frequency domain function which is comprised of sinusoids with specific amplitude and phase characteristics. The squared magnitude of a response as a function of frequency (auto power spectrum) can be obtained as follows:

$$S_{yy}(j\omega) = Y^*(j\omega) \cdot Y(j\omega) \quad (1)$$

where $Y(j\omega)$ is the Fourier transform of a response time history and $Y^*(j\omega)$ is the complex conjugate of $Y(j\omega)$. If the input force time history ($x(t)$) is also measured, a cross power spectrum can be computed:

$$S_{xy}(j\omega) = X^*(j\omega) \cdot Y(j\omega) \quad (2)$$

The amplitude and phase relationship between the response and a given input is used to define a system transfer function (complex frequency response function) as follows:

$$H(j\omega) = \frac{Y(j\omega)}{X(j\omega)} = \frac{X^*(j\omega) \cdot Y(j\omega)}{X^*(j\omega) \cdot X(j\omega)} = \frac{S_{xy}(j\omega)}{S_{xx}(j\omega)} \quad (3)$$

The use of the cross spectrum and input auto spectrum removes the need for complex division, and, more importantly, the cross spectrum tends to improve transfer function estimates by removing the effects of noise that is not correlated with the input force.

The Fourier transform of the transfer function is the impulse response function, which is a time history comprised of damped sinusoids that indicate structural response to an impulse type of input. The frequency, damping, amplitude, and phase of the sinusoids that make up the impulse response function (or complex frequency response function) define the modal characteristics of the structure at the measured location for a specific flight condition.

Modal analyses of these transfer functions or impulse response functions are being made in the technical community in many different ways. Some methods use minicomputers, some larger computers. Much of the AFFTC analysis capability is based on a Time/Data 1923/50 Time Series Analyzer and the associated Modal Analysis (Laplace) Package software. Some of the techniques discussed in this paper are specific to this software package. The overall AFFTC analysis capability attempts to capitalize on the strengths and compensate for the limitations of each software component so that the final flutter clearance is as rapid and accurate as possible.

The determination of the system transfer function is of fundamental concern. The software subroutine package used permits modal analysis when the input and output time histories are measured and when the structural response alone is measured. Aircraft responses excited by pilot-induced control surface impulses have been analyzed without knowing the true forcing input.

It is assumed that the response in the response only case is characteristic of a minimum phase system. This implies that the system is physically realizable, that damping is stable for all modes, and that of all the impulse responses with the same autocorrelation, the one selected has the most rapid initial buildup of energy. When these conditions are met, a form of the Hilbert transform can be used to calculate the minimum phase of the system given only its amplitude characteristics. (The minimum phase calculations are described and compared with the more common autocorrelation technique in the appendix.) To calculate the transfer function accurately directly from the derived minimum phase spectrum, $Y'(j\omega)$, an additional assumption is made as follows:

$$H(j\omega) = \frac{Y'(j\omega)}{X(j\omega)} \quad (4)$$

where $X(j\omega)$ is a constant. The input forcing function has a constant amplitude frequency power spectrum in the frequency band of interest. This is characteristic of impulse, random noise, and swept sine wave inputs. In reality, the input spectrum is not perfectly flat, but the assumption still produces reasonable accuracy, and the merit of the technique has been proven in flight test. If the input is not flat, the response may indicate high energy at a location that corresponds to a pole of the drive function. This possibility must be considered by the engineer because it occurs in all techniques of response only analysis.

If the input forcing function can be measured, it is better to use the transfer function estimate obtained from equation (3). The transfer function estimate, whether calculated directly or by using the minimum phase concept, contains the modal information which is extracted during the Laplace analysis.

The Laplace analysis uses the concept of a partial fraction expansion of the complex frequency response function to define modal parameters for each pole, $s = s_i$, in the Laplace plane, as follows:

$$\begin{aligned}
 H(j\omega) &= H(s) = \sum_i \left\{ \frac{r_i^*}{s + s_i^*} + \frac{r_i}{s + s_i} \right\} \\
 &= \sum_i \left\{ \frac{R_i e^{j\theta_i} (\pi/180)}{s + (2\pi\alpha_i - j2\pi k_i)} + \frac{R_i e^{-j\theta_i} (\pi/180)}{s + (2\pi\alpha_i + j2\pi k_i)} \right\} \quad (5)
 \end{aligned}$$

A graphical description of the poles and the related modal parameters is given in figure 3. The pole location, s_i , defines the absolute damping, α_i , and the frequency line number, k_i , of the mode. The numerator in equation (5), r_i , is a complex residue composed of a magnitude, R_i , and a phase, θ_i . This residue defines the modal eigenvector when measurements are made over an entire structure. For structures with nonproportional damping, the residue defines a complex mode; but for modes with proportional damping, the phase relationships of the eigenvector points only differ by approximately 0° or 180° . The impulse response function in the form derived by the Laplace software demonstrates the physical meaning of the modal parameters:

$$h(t) = \sum_i \{ 2R_i e^{(-2\pi\alpha_i)t} \cos [2\pi k_i t + \theta_i (\pi/180)] \} \quad (6)$$

The absolute damping and the frequency line number can be related to the more familiar damping ratio, ζ , or structural damping, g , and frequency, f , as follows:

$$\zeta = \frac{1}{2} g = \alpha \frac{1}{\sqrt{k^2 + \alpha^2}} \quad (7)$$

$$\approx \frac{\alpha}{k} \text{ for lowly damped modes}$$

$$f = \frac{(k) \text{ (sample rate)}}{(\text{frame size})} \text{ Hz} \quad (8)$$

A description of the theory of defining modal parameters in terms of the Laplace plane and an explanation of the validity of the partial fraction expansion of the transfer function in terms of poles and residues is to be found in reference 1. Reference 1 also discusses the concept of nonproportional damping. The algorithm that is actually used to transfer mathematically from the Fourier representation of a system to the Laplace plane (fig. 3) is currently proprietary information. An intuitive verification of the technique can be made, however, by observing that the impulse response in equation (6) can be defined by using the superposition of the Laplace parameters. The use of such a mode generation approach has made it possible for engineers to generate known functions digitally and to perform circle checks on the modal results calculated from the transfer function.

The Laplace software contains procedures that attempt to identify the modes which have the highest spectral energy and the lowest damping. A modal energy value is calculated for each pole as a percentage of total energy in the frequency band being analyzed. Only the modes with a percentage energy greater than a selected cutoff value and with an attenuation (absolute damping) less than a specified cutoff are included in the mode list print-out. This procedure eliminates long mode list printouts and makes it much easier for the analyst to identify and track the modes that are of interest to him.

The accuracy of the Laplace algorithm and its ability to separate closely spaced modes has been investigated at AFFTC by using digitally generated transfer functions. Single or bipolar modal parameter lists were input, a complex transfer function was derived, the Laplace routines calculated the modal parameters, and a comparison was made between input data and the extracted data in order to assess program limitations. The single mode study verified that frequency was derived accurately and that damping was calculated to within 10 percent of the correct value for the modes with viscous damping ratios less than 0.10, except for modes near the upper cutoff frequency. A typical error envelope showing the maximum values of damping which resulted in a 10-percent error in damping is shown in figure 4. The attenuation curve demonstrates that the interference effect of the ends of the data frame can be significant. Knowledge of this effect and the relationship between damping ratio and absolute damping (eq. (7)) is used by the analyst to insure that appropriate frame sizes and sampling rates are selected in order to extract the modes of interest accurately.

The bipolar digital complex frequency function study used a parametric variation of damping ratio and frequency resolution

element separation. The separation in hertz, Δf , between resolution elements k_i and k_{i+1} is

$$\Delta f = \frac{1}{\Delta t}, \quad (9)$$

where Δt is the time in seconds contained in the data frame prior to performing the Fourier transform. Damping ratio was varied from 0.005 to 0.10 and frequency separation was in the range of 1 to 160 elements in a complex frequency domain frame of 256 lines. The following results were obtained:

- (1) Accuracy of the frequency and damping ratio estimates increased as the separation between the two modes increased.
- (2) The error in the calculation of the characteristics of modes with low damping ($\zeta < 0.035$) was less than 10 percent. A five-resolution-element separation between modes was the minimum necessary to consistently maintain this accuracy.
- (3) As two modes converged in frequency, the accuracy of the estimates was degraded. Lightly damped modes ($\zeta < 0.035$) were evaluated accurately regardless of the presence of other modes. Estimates of closely spaced modes which had higher damping were in error, but the accuracy of the estimate improved if both modes were highly damped.

The digital studies verified that all significant modes (sufficient energy and low damping) would be accurately identified by the Laplace software from a given transfer function. (The highly damped modes were of minor concern to AFFTC engineers during a real-time flight test clearance program. When desired, these modes were analyzed separately by using more appropriate techniques.)

The Laplace package software was also evaluated by using analog computer models. Table 1 shows the results of a four-mode case in which a pulse excitation was used. These response only cases were analyzed by using the minimum phase algorithm before performing the Laplace analysis. The frequency was generally accurately determined for well excited modes when damping ratios were less than 0.20. The analyst used the frequency response magnitude plots to verify the estimates visually. The frequency and damping values were determined accurately for modes that were well within the design envelope of the Laplace software ($\zeta < 0.10$). The highly damped modes often exhibited low calculated damping values (on the order of 0.001), although this error was readily apparent to the engineer by observing the transfer function magnitude plots. The false modes were also identified by observing their low energies and/or low residues on the mode list printout.

Analog models were also used to verify the system's accuracy for swept sine wave results. A unique approach reported in reference 2 has been employed to reduce truncation errors encountered when the sweep time is too long (core is too restricted) to be included in one frame of data. The traditional approach in averaging has been to ensemble average data in the frequency domain. (If multiple frames of data are required, take the FFT of each frame and frequency average the multiple frequency domain results.) As shown in figure 5, a mode's response may be truncated by a frame. This results in erroneous modal parameter estimates. The new approach, which is called time averaging at AFFTC, uses the fact that the frequency content is continually changing so that multiple time histories can be superimposed without distorting the earlier portions of the time history. The periodic nature of the FFT (fig. 6) permits the entire swept sine wave response to be averaged without truncation errors because all the time segments are still represented in the time history that is Fourier transformed. The repeating signal at the top of figure 6 can be added to the repeating signal in the middle of figure 6 (the second frame in the sweep in fig. 5), and the result (at the bottom of fig. 6) appears to be two segments of data of length $2T$ which are superimposed after being shifted with respect to each other by $1T$. The total frame length being transformed is T , and this is the value that determines the frequency resolution. This procedure would not be accurate if the same frequency content occurred in multiple frames - if, for example, noise significantly excited the modes. A good procedure in this instance is to include the entire mode response within one data frame so that there is no response truncation and minimal noise interference. Typical Laplace results for a swept sine wave model are provided in figure 7 for the two types of averaging.

The digital and analog simulations demonstrated to AFFTC engineers that the Laplace package software was well suited to the evaluation of critical modes in flutter testing. A multimode response could be analyzed without knowing where the modes were in advance, and all nonhighly damped modes would be extracted simultaneously with good accuracy. The pulse type of response only data was evaluated well by using the minimum phase concept to generate the phase of the transfer function.

FLIGHT FLUTTER TEST APPLICATIONS AND RESULTS

The use of digital time series analysis techniques in flight tests verified the advantages of the AFFTC system and

reminded the engineers of the limitations inherent in all time series analysis methods. The system was used in the testing of a number of different aircraft types with different excitation systems. Tests of the F-111 transonic aircraft technology (TACT) vehicle and a B-52D aircraft configured with various external stores used pilot-induced control surface pulses, tests of the A-10 airplane used aerodynamic vane exciters, and the tests of the B-1 air vehicle used dynamic mass exciters. The actual analysis techniques used in these programs varied somewhat depending on the modes of interest and the testing conditions.

Typical hard copy output for a test in which control surface pulses were used is shown in figures 8 and 9 and table 2. The AFFTC software was written to utilize the Laplace software package subroutines efficiently during a real-time flutter analysis. Figure 8 contains a time history of sampled response data for an elevator pulse during a B-52D aircraft/store certification program. The dashed lines indicate the 6.25 seconds of data which were analyzed by using the minimum phase assumption. The maximum response peak was used as a starting location because it resulted in more consistent data trends. (The pilot input did not result in a true spike input because the dynamics of the control system caused small overshoot oscillations.) The magnitude of the transfer function is shown in figure 9. The engineer could also view the coincident, quadrature, or phase spectrums or phase plane plots. The vertical lines in figure 9 were drawn automatically at frequencies selected for analysis by the Laplace software. The analyst then had the opportunity to change the frequency analysis band, damping (α) cutoff, and energy threshold; or he could have the mode list (table 2) displayed and copied. If the input was known, the time history would not normally be displayed and the minimum phase assumption would not be needed to derive the transfer function; but the rest of the analysis would be the same.

In table 2, the damping levels of the 4.16-hertz and 5.76-hertz modes would be questioned by the analyst because of low energies and residues (poor excitation). It is significant that two high energy, high residue, closely spaced modes were identified. The frequency and damping of these modes could not be determined easily by using traditional strip chart logarithmic decrement analyses. The total time required to perform the analysis and obtain the hard copy results shown was 1.1 minutes. Additional time histories were analyzed from disk data as desired. Multiple data trends were plotted by hand during the flight, but mode results stored on the disk were plotted during postflight sessions using the graphics display unit and its hard copy device. These hard copy outputs permitted efficient

postflight data review and reduced the number of man-hours required to generate an accurate final report.

Resolution and Record Length

A limitation encountered in the time series analysis of structural response data whether digital or analog methods are used is the relation between frequency resolution and record length (eq. (9)). In the stick rap response data above, the resolution, Δf , was 0.16 hertz because only a 6.25-second time frame was filled with data before the signal decayed to the noise level. The response signature for modes with higher damping or higher frequencies may be considerably shorter than in the example, and the resolution would end up by being lower. (If the frame size is not shortened appropriately, the data appear to have lower damping because of the continuously excited data in the noise level and statistical variability.)

As demonstrated in figure 10, the reduction in resolution has several effects on the data: (1) the data curves are smoothed and less noise is evident; (2) the ability to separate closely spaced modes decreases; and (3) the minimum damping level which can be defined increases. The last effect could be catastrophic in flutter testing.

Signal To Noise Ratio

The resolution problem intensifies when the signal to noise ratio in flight testing is degraded. When this happens some smoothing of the data is necessary. However, the effective frequency resolution then decreases. Both higher force levels and longer sweep times are used to improve the signal to noise ratio. The calculation of the transfer function depends on the correct measurement of input and output. If the aircraft is excited significantly by turbulence or buffet, the measured input is wrong; therefore, the estimate of the transfer function is wrong, and this distorts the modal parameter calculations.

In figure 11, the signal to noise ratio in the response is poor. The aircraft was power limited at its high speed flutter points, so the linear sweep times were restricted to 7 seconds. The transfer function for this time history is shown in figure 12. Most of the energy in figure 12 is in a symmetric mode (between the dashed lines), but the structure was being excited anti-symmetrically by aerodynamic vanes. The poor transfer function estimate prevented the antisymmetric mode of interest from being analyzed accurately by the software. The engineers used the

bandpass filters and the reliable frequency dwell/quick stop methods to track the mode of interest. Better estimates of the true transfer functions were obtained when the signal to noise ratio improved, and the Laplace technique then generally gave reasonable results. Dwell/quick stop methods were also used to obtain damping estimates for modes of interest which exhibited energy levels which were too low for accurate digital analysis.

The technique of adding or subtracting channels of data to emphasize symmetric or antisymmetric modes has been used with some success on data similar to those shown in figures 12 and 13. The resulting signal to noise ratio improved in that only the modes of interest were included, but the buffet response in the mode of interest also increased. The process was useful while a minimum phase analysis was used to identify modes, but the direct calculation of the transfer function was still in error because of the multiple inputs.

Random Noise Excitation

The flexibility of the minicomputer-based analyzer permits the engineer to select alternative analysis techniques if required. During the F-111 TACT program, transonic buffet excited modes with frequencies which were higher than the frequencies being excited by the stick raps. The Laplace software, working with a 5-second sample of data which followed the stick rap, would identify the higher modal frequencies, but the calculated damping level would be low because of the continuous excitation during the sampling. These modes were analyzed during postflight sessions by using the waveform-averaging capability of the analyzer to generate a randomdec signature.

The randomdec analysis, a technique developed by Henry Cole, Jr. (ref. 3) uses 30 to 45 seconds of buffet response to generate a pseudo impulse response function. As figure 13 shows, the impulse response characteristics of the 16.7-hertz mode could readily be identified. When a minimum phase analysis was applied to the response spectrum generated over the same time period as was used to calculate the randomdec signature (fig. 13), the calculated damping was low. The frequency-ensemble-averaged auto-spectrum did not have enough averages to reduce the statistical variability. The noise spikes in the power spectra would be identified as lightly damped modes by the software. Smoothing the data reduced the effective resolution of the data to unacceptable levels. The analog randomdec technique was not used in real time because the analyst would have been limited to one response channel and one frequency. The stick raps excited the modes of interest from a flutter standpoint (approximately 5 hertz and

7 hertz) and the analyses were done on multiple channels in nearly real time.

A digital version of the randomdec process has been written recently, so multiple channels and frequencies can be analyzed from the time histories stored on disk. The technique will be used in selected analyses, but it still has difficulty in separating closely space modes and it is sensitive to bandpass filter bandwidth.

CONCLUDING REMARKS

The use of digital time series analysis techniques at the Air Force Flight Test Center (AFFTC) has been beneficial in terms of time and accuracy. The Modal Analysis (Laplace) Package software proved to be a valuable tool for analyzing transfer functions which had been calculated either from known inputs or from minimum phase response spectra. Of particular value was the ability of the Laplace method to analyze significant, lightly damped modes even when the modes were closely coupled. The engineer needed a working knowledge of both aeroelasticity and time series analysis to analyze flutter test data, but he did not need to know the location or the number of the significant modes before the analysis. (Prior knowledge does make things easier, however.) The AFFTC minicomputer-based system is a tool that is flexible and low in cost (in terms of initial investment and reduced test time), and it can easily be reprogramed as new algorithms are developed.

The limitations of the analysis are related to record length, signal to noise ratio, and measurement of frequency response functions. New techniques of noise reduction and transfer function enhancement are being studied at AFFTC as well as at many other places. The effective use of turbulence- or buffet-excited response data is also being pursued.

The mission of AFFTC and the requirements this mission sets for a real-time flutter test analysis system mean that the approach taken must be general and that the technique must be cost effective. The use of digital time series analysis techniques at AFFTC during the last 3 years has been helpful in clearing aircraft quickly and safely and has also been very instructive in the proper use of these methods. The engineers at AFFTC expect the implementation of improved digital techniques to result in even greater benefits during future flutter testing.

APPENDIX

COMPARISON OF MINIMUM PHASE CRITERIA WITH THE AUTOCORRELATION APPROACH

For certain conditions, there is a definite one-to-one relationship between the frequency response characteristics P and Q where

$$H(j\omega) = P(\omega) + jQ(\omega) = A(\omega)e^{j\phi(\omega)} \quad (A1)$$

The amplitude, $A(\omega)$, and the phase, $\phi(\omega)$, are uniquely related to the real and imaginary components of the transfer function:

$$A(\omega) = \sqrt{P^2(\omega) + Q^2(\omega)} \quad (A2)$$

$$\phi(\omega) = \arctan \left(\frac{Q(\omega)}{P(\omega)} \right) \quad (A3)$$

It can be noted that the logarithm of the transfer function is related to the log amplitude characteristic and the phase characteristic in the same manner that $H(j\omega)$ is related to P and Q in equation (A1).

$$\ln H(j\omega) = \ln (A(\omega)) + j\phi(\omega) \quad (A4)$$

If the system is both stable and causal, Hilbert transforms can be derived which relate P and Q (ref. 4):

$$P(\omega) = -\frac{1}{\pi} \int_{-\infty}^{\infty} \frac{Q(u)}{u - \omega} du \quad (A5)$$

$$Q(\omega) = \frac{1}{\pi} \int_{-\infty}^{\infty} \frac{P(u)}{u - \omega} du \quad (A6)$$

The similarity of equations (A1) and (A4) makes it possible to calculate either the amplitude or phase given the other. In this case, the logarithm of $H(j\omega)$ must have neither unstable poles nor zeroes.

$$\ln A(\omega) = -\frac{1}{\pi} \int_{-\infty}^{\infty} \frac{\phi(u)}{u - \omega} du \quad (A7)$$

$$\phi(\omega) = \frac{1}{\pi} \int_{-\infty}^{\infty} \frac{\ln A(u)}{u - \omega} du \quad (A8)$$

Of more practical interest in calculating the phase in digital studies is the following equation, which utilizes the Fourier transform (ref. 5).

$$\phi(\omega) = \text{DFT} \left\{ \left\{ \frac{1}{2} - U\left(t - \frac{T}{2}\right) \right\} \cdot \left\{ \text{IFT}(\ln S_{yy}(\omega)) \right\} \right\} \quad (A9)$$

where

DFT direct Fourier transform,

IFT inverse Fourier transform, and

T arbitrary time in the data frame with the fundamental Fourier period going from 0 to T

$$\frac{1}{2} - U\left(t - \frac{T}{2}\right) = \begin{cases} +\frac{1}{2} & 0 < t < \frac{T}{2} \\ 0 & t = 0, \frac{T}{2}, T \\ -\frac{1}{2} & \frac{T}{2} < t < T \end{cases}$$

The $\phi(\omega)$ which is calculated is known as a minimum phase, and the system is a minimum phase system. The complete frequency response function is estimated by combining the minimum phase with the square root of the autospectrum. The frequency response may then be inverse Fourier transformed to give the true impulse response function for the minimum phase system.

Three assumptions must be made about the data for the minimum phase procedure to be used. First, it is assumed that all modes have stable damping. Second, the system is assumed to be causal; that is, the impulse response is considered to be zero for negative time and it is assumed that the system cannot respond to an input before it occurs. Third, of all frequency responses with the same autospectrum, the one selected is assumed to have the smallest total change in phase angle from zero to maximum frequency. This implies that, of all impulse responses with the same autocorrelation, the one selected has the most rapid initial buildup of energy.

The first two criteria would almost certainly be true in an aircraft response. The third criterion is more difficult to verify for a particular structural response, but the minimum phase

usually approximates the true impulse response better than the zero phase imposed during an autocorrelation. If the structural response builds up to its maximum amplitude quickly (an estimate is less than 1 cycle) when subjected to an impulse, the minimum phase assumption should be valid. If the buildup is slow (several cycles), the results of the minimum phase procedure are probably invalid. The frequency and damping obtained from the impulse response would still be correct, but the amplitude would be incorrect.

If the system does comply with the previous criteria, the autocorrelation and the autospectrum of the minimum-phase-estimated complete frequency response are exactly the same as the autocorrelation and autospectrum of the true frequency response. The results of the minimum phase procedure can be compared with the results of the autocorrelation technique. The autocorrelation of an impulse response is not always equal to the impulse response, and the derivative of the autocorrelation of an impulse response is not always equal to the impulse response. An explanation of the autocorrelation and the derivative of the autocorrelation can be found in reference 6.

As shown in reference 6, a simple damped mass system with sine phase will have the following impulse response:

$$h_1(t) = \frac{1}{mb} e^{-at} \sin bt \quad (A10)$$

where m is mass, $b = \omega \sqrt{1 - \zeta^2}$, and $a = \omega\zeta$.

If a cosine phase function is defined, a second impulse response can be determined as follows

$$h_2(t) = \frac{1}{mb} e^{-at} \cos bt \quad (A11)$$

and the autocorrelation of these two functions can be calculated:

$$\begin{aligned} C_1(\tau) &= \frac{e^{-a\tau}}{4m^2 a \omega^2} [\cos(b\tau) + \frac{a}{b} \sin(b\tau)] \\ &= \frac{1}{4m\omega^2} h_1(\tau) + \left(\frac{b/a}{4m\omega^2}\right) h_2(\tau) \end{aligned} \quad (A12)$$

$$C_2(\tau) = \frac{e^{-a\tau}}{4m^2a\omega^2} \left[\left(1 + 2\frac{a^2}{b^2}\right) \cos(b\tau) - \frac{a}{b} \sin(b\tau) \right]$$

$$= \frac{\left(1 + 2\frac{a^2}{b^2}\right) \frac{b}{a}}{4m\omega^2} h_2(\tau) - \frac{1}{4m\omega^2} h_1(\tau) \quad (A13)$$

The derivative of these autocorrelations can also be written as follows:

$$\dot{C}_1(\tau) = -\frac{1}{4ma} h_1(\tau) \quad (A14)$$

$$\dot{C}_2(\tau) = \frac{-1}{2mb} h_2(\tau) - \frac{1}{4ma} h_1(\tau) \quad (A15)$$

As noted in reference 6, $\dot{C}_1(\tau)$ is equal to, within a constant, $h_1(t)$. If a new function is now defined such that c_1 and c_2 are the following constants

$$h_3(t) = c_1 h_1(t) + c_2 h_2(t) \quad (A16)$$

the following autocorrelation and autocorrelation derivative equations can be obtained:

$$C_3(\tau) = c_1^2 C_1(\tau) + 2c_1 c_2 \frac{a}{b} C_1(\tau) + c_2^2 C_2(\tau) \quad (A17)$$

$$\dot{C}_3(\tau) = c_1^2 \dot{C}_1(\tau) + 2c_1 c_2 \frac{a}{b} \dot{C}_1(\tau) + c_2^2 \dot{C}_2(\tau) \quad (A18)$$

It is evident from equations (A17) and (A18) that while the attenuation and oscillation rates of an unknown impulse response are uniquely determined without knowing the phase by calculating the autocorrelation or the derivative of the autocorrelation, the amplitude cannot be determined except for a very lightly damped impulse. It has also been found that the autocorrelation, or its derivative, of the particular impulse response is not always proportional to the impulse response.

The derivation of the system parameters from the response only cannot be expected to give as good an answer as can be obtained when the input and output are used. However, the autocorrelation method and the minimum phase approach often give reasonably accurate estimates of frequency and damping. An advantage of using the minimum phase assumption, when it is applicable, is that the mode shape (with the exception of a possible

180° phase shift) can be determined for modes with proportional damping. For complex modes, both the autocorrelation and the minimum phase mode shape estimates are distorted, but the latter estimate is better.

REFERENCES

1. Hurty, Walter C.; and Rubinstein, F.: Dynamics of Structures. Prentice-Hall, Inc., 1964.
2. Norin, R. S.; and Sloane, E. A.: A New Algorithm for Improving Digital Random Control System Speed and Accuracy. Proceedings of the 21st Annual Technical Meeting of the Institute of Environmental Sciences, Volume 2, 1975, pp. 46-52.
3. Cole, Henry A., Jr.: On-Line Failure Detection and Damping Measurement of Aerospace Structures by Random Decrement Signatures. NASA CR-2205, Mar. 1973.
4. Solodovnikov, V. V. (W. Chrzczonowicz, transl.): Statistical Dynamics of Linear Automatic Control Systems. Second ed. Van Nostrand Reinhold Co., 1965.
5. Oppenheim, Alan V.; and Schafer, Ronald W.: Digital Signal Processing. Prentice-Hall, Inc., 1975.
6. Houbolt, John C.: Subcritical Flutter Testing and System Identification. NASA CR-132480, Aug. 1974.

TABLE 1.- MODEL COMPARISON FOR FOUR MODE CASES
WITH EQUIVALENT PULSE EXCITATION.

CASE NO.	MODEL EXCITATION	MODE 1		MODE 2		MODE 3		MODE 4		TYPE OF SIGNAL
		f_1	ζ_1	f_2	ζ_2	f_3	ζ_3	f_4	ζ_4	
----	MODEL	3.0	.050	6.0	.020	8.0	.10	12.0	.200	----
17	$\dot{X}_1(0) - \dot{X}_2(0) = .5v$	3.0	.0526	6.0	.0222	7.40	.0362	-	-	DISPLACEMENT
	$\dot{X}_3(0) - \dot{X}_4(0) = 1.0v$	3.0	.0510	6.0	.0192	8.40	.0293	-	-	VELOCITY
18	$\dot{X}_1(0) - \dot{X}_2(0) = .25v$	3.0	.0510	6.0	.0206	7.79	.0600	-	-	DISPLACEMENT
	$\dot{X}_3(0) - \dot{X}_4(0) = .5v$	3.0	.0594	6.0	.0198	7.79	.0338	11.8	.0044	VELOCITY
19	$\dot{X}_1(0) - \dot{X}_2(0) = .125v$	3.0	.0505	6.0	.0198	7.79	.0654	-	-	DISPLACEMENT
	$\dot{X}_3(0) - \dot{X}_4(0) = .25v$	3.0	.0578	6.0	.0197	7.79	.0364	11.6	.0092	VELOCITY
20	$\dot{X}_1(0) - \dot{X}_2(0) = .062v$	3.0	.0476	6.0	.0205	8.20	.0572	-	-	DISPLACEMENT
	$\dot{X}_3(0) - \dot{X}_4(0) = .125v$	3.0	.0636	6.0	.0193	7.99	.0304	-	-	VELOCITY

TABLE 2.- AFFTC FLUTTER TEST RESULTS:
MODE LIST PRINTOUT.
(27,000 ft = 8239 m)

RUN NO. = 18

SPEED = 350.E

ALTITUDE = 27000

X-DUCER = 7.

SETUP NUMBER = 1

ENRG. THRES. = .01

ALPHA CUTOFF = 25.6

% TOT. ENERGY = .9789

MODE NO:	% ENERGY:	FREQ:	S-DAMP:	RESIDUE:	PHASE:
1.	28.73	2.24	.0967	1.511	-79.78
2.	69.15	3.04	.0536	1.756	-76.61
3.	1.038	4.16	.0507	.2792	-58.11
4.	1.072	5.76	.0447	.3597	-134.3

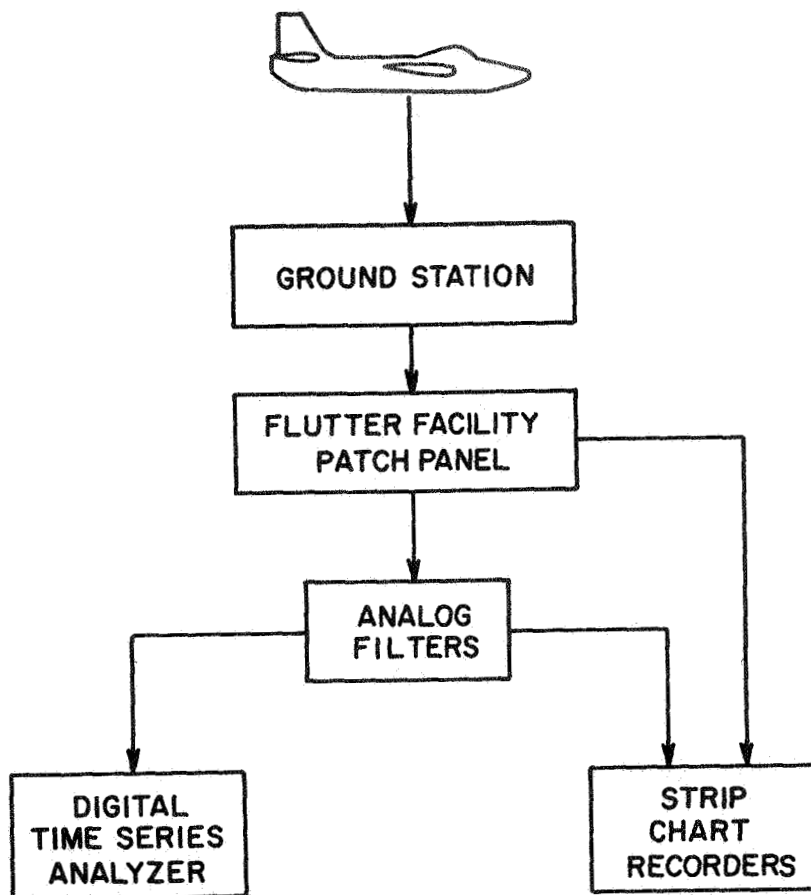


Figure 1.- Flutter test data flow,



Figure 2 - APPTC flutter facility equipment.

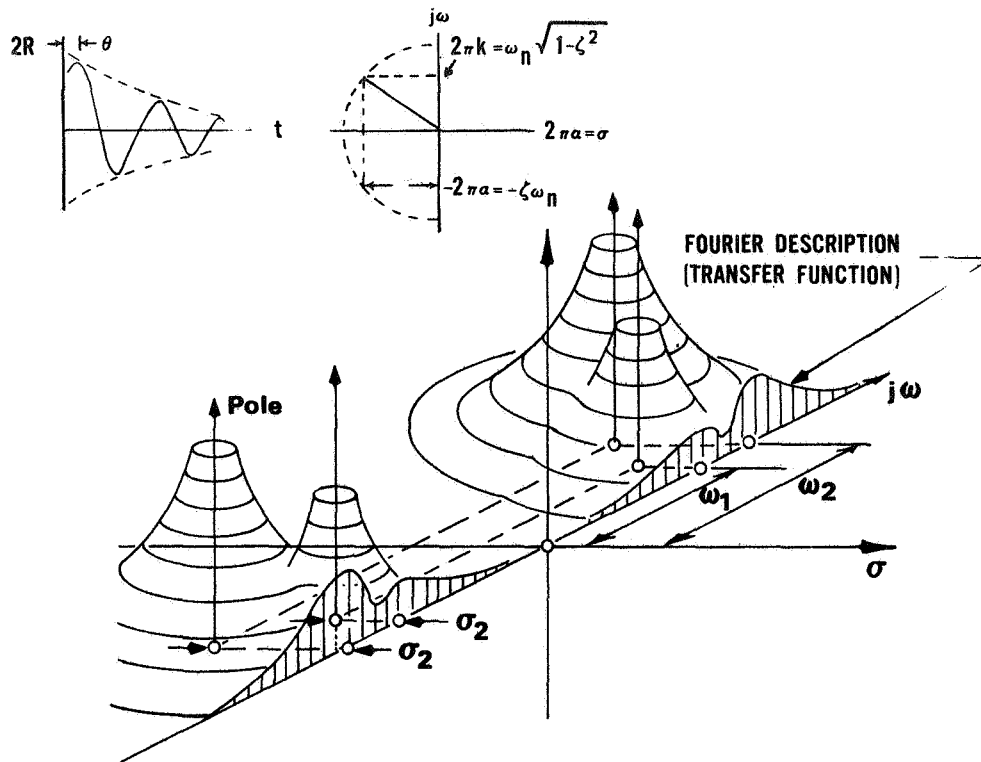


Figure 3.- Transfer function parameters.

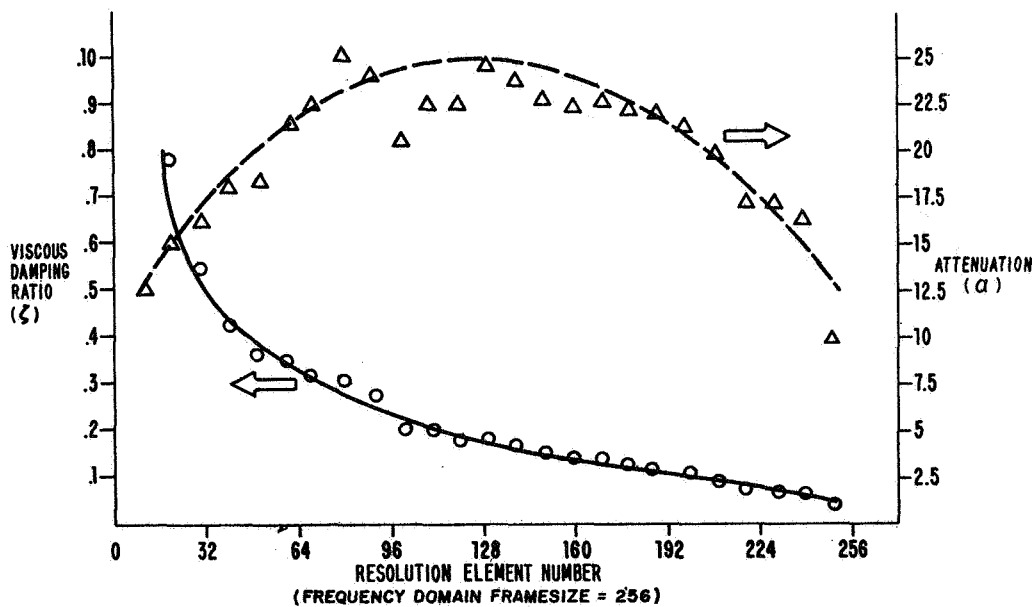


Figure 4.- Ten-percent error limitation plot.

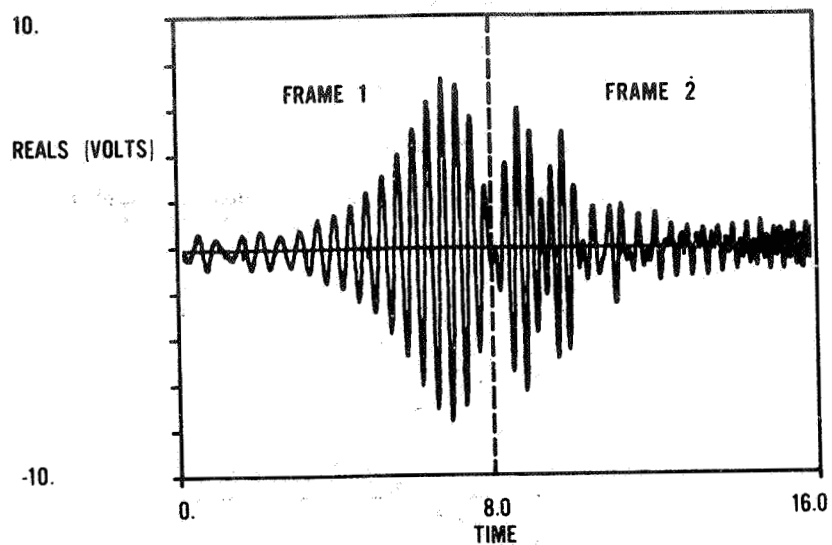


Figure 5.- Truncation of data frames.

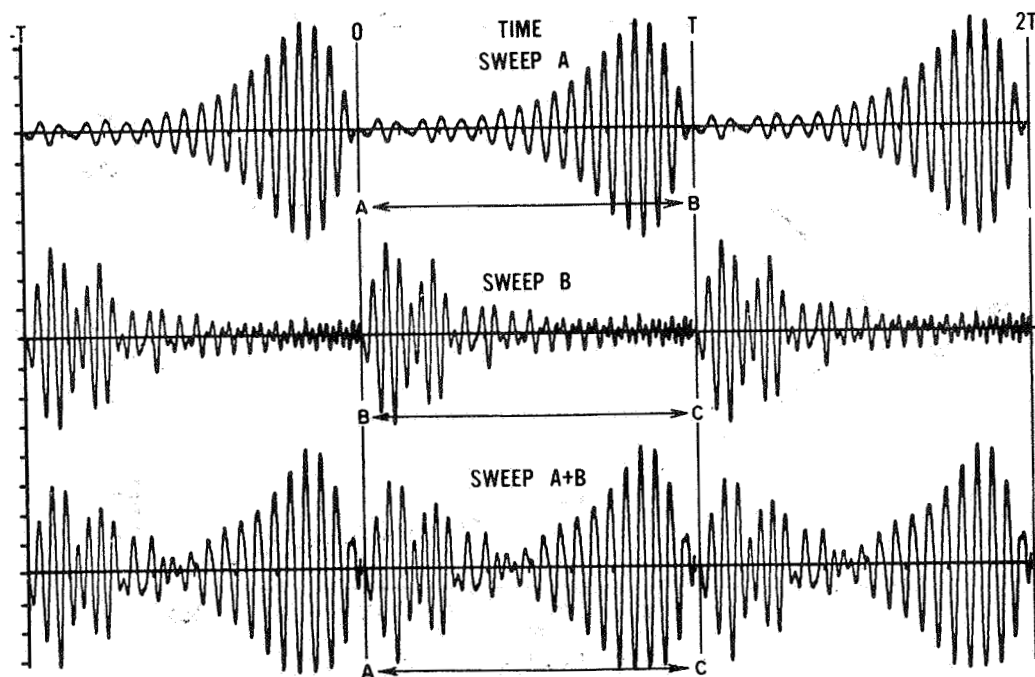
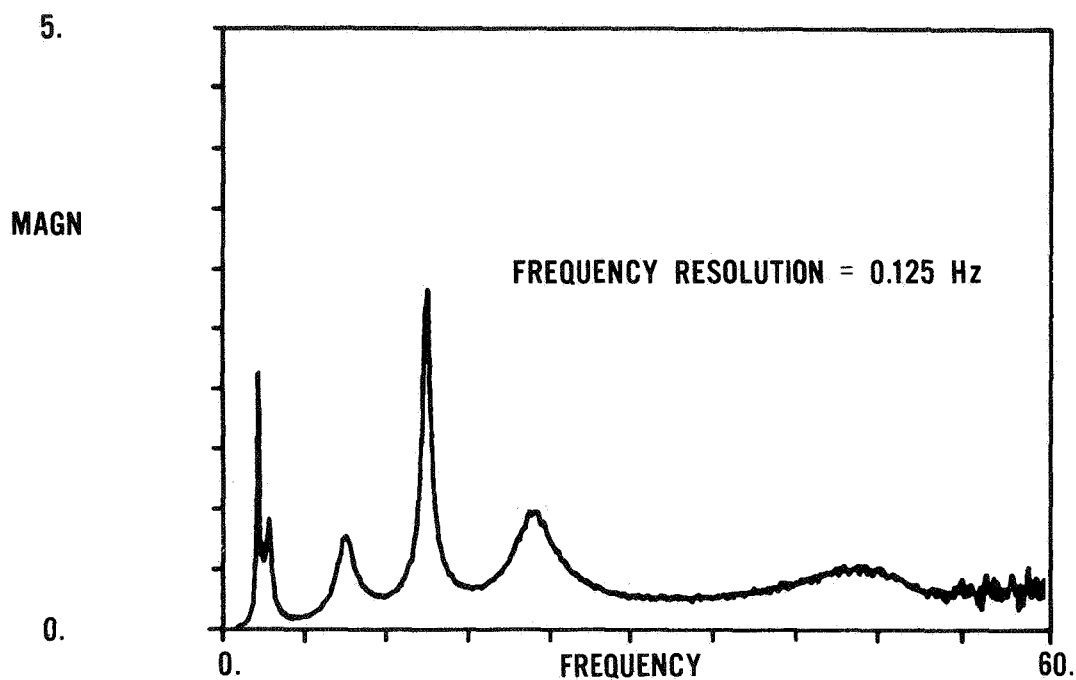


Figure 6.- Time averaging.



• MODEL PARAMETERS

FREQUENCY	STRUCTURAL DAMPING
2.56	.040
3.34	.103
8.79	.119
14.74	.032
22.27	.119
45.80	.204

• COMPUTED PARAMETERS

TIME AVERAGING		FREQUENCY AVERAGING	
FREQUENCY	S-DAMPING	FREQUENCY	S-DAMPING
2.62	.0423	2.62	.0915
3.37	.107	3.37	.0873
8.75	.072+	8.87	.03+
15.0	.0319	15.0	.0363
22.5	.03+	22.25	.018+
—	—	—	—

Figure 7.- Analysis of model data using swept sine input.

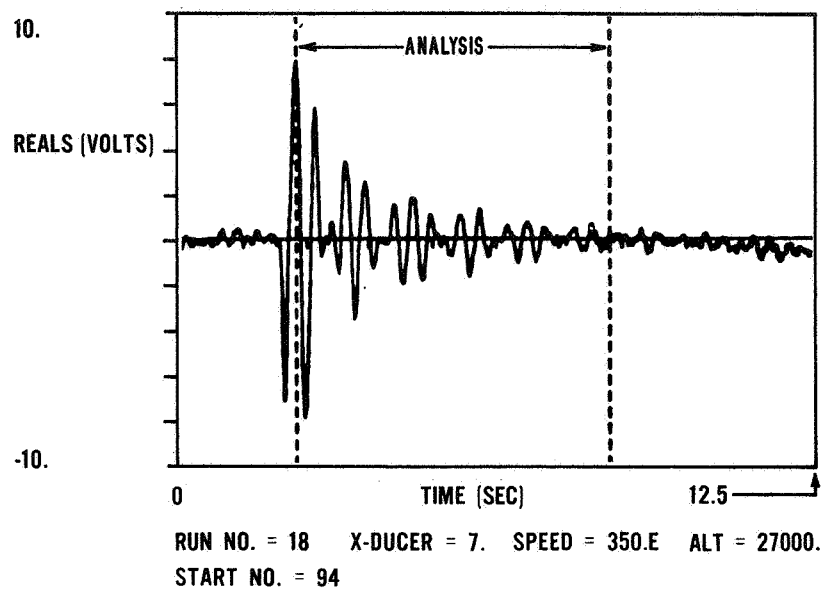


Figure 8.- AFFTC flutter test results:
time history selection.
(27,000 ft = 8230 m)

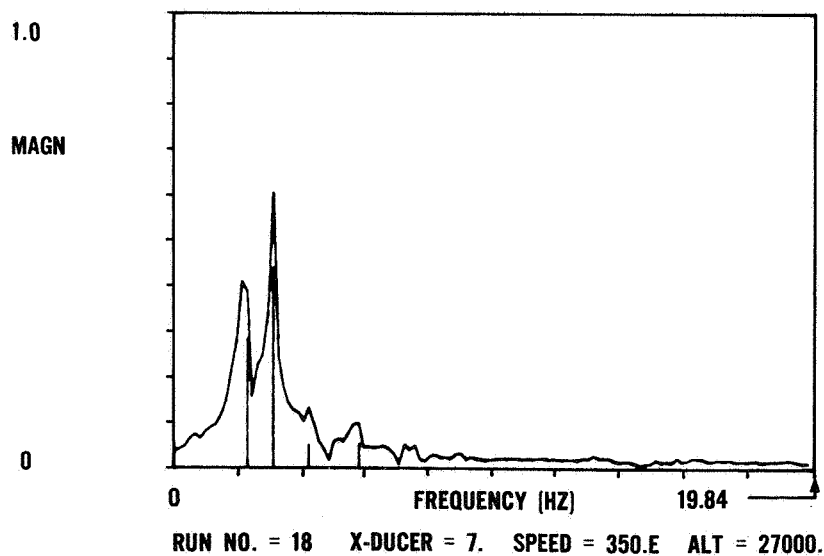


Figure 9.- AFFTC flutter test results:
transfer function magnitude.
(27,000 ft = 8230 m)

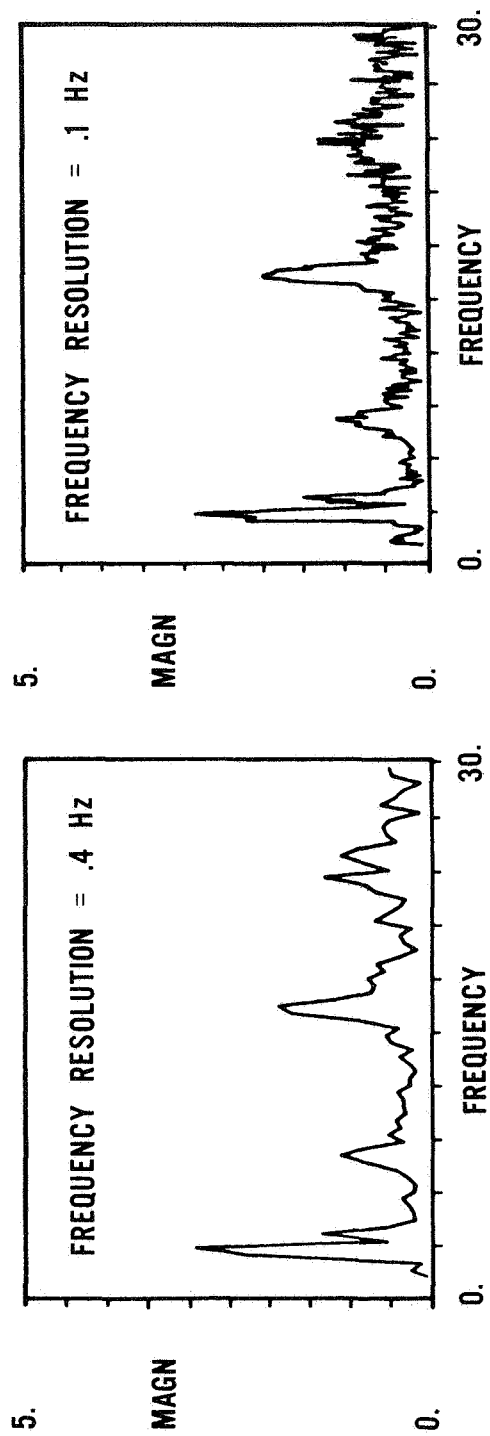


Figure 10.- Relationship between frequency resolution and data smoothing.

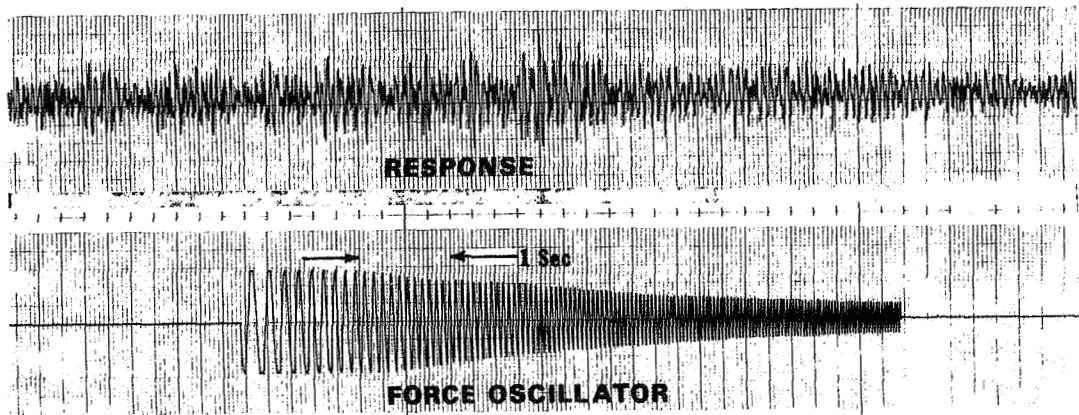


Figure 11.- Forced response in the presence of noise.

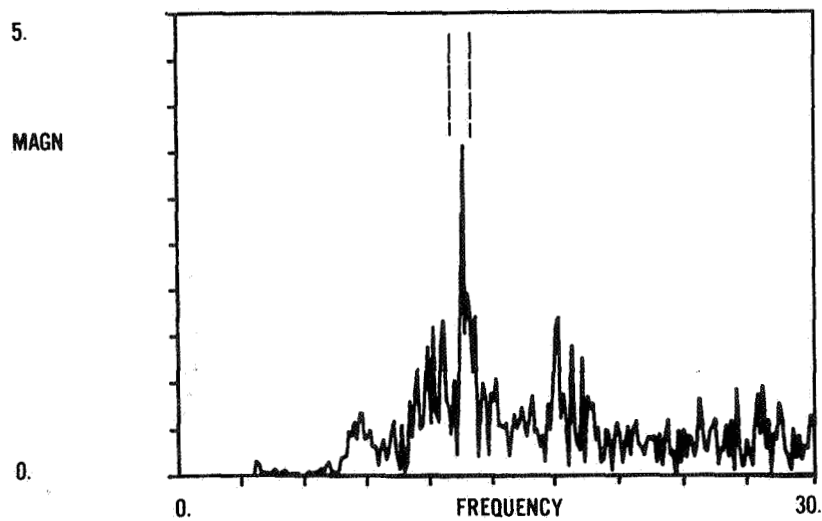
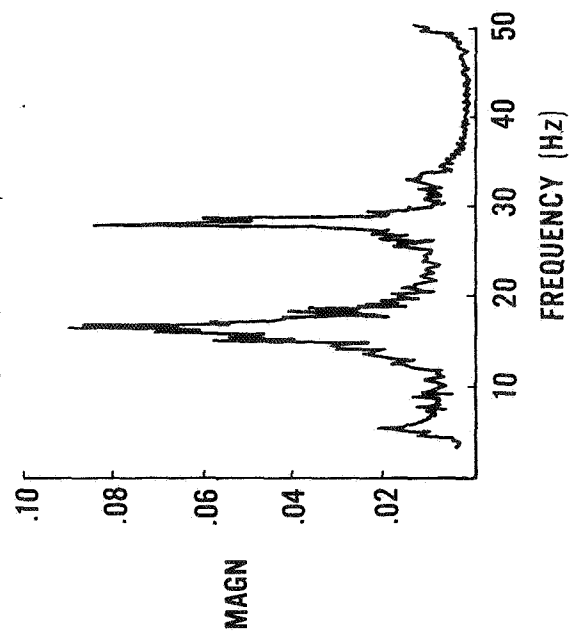


Figure 12.- Magnitude of the transfer function for a forced response in the presence of noise.

AUTOSPECTRUM

MACH NUMBER = 0.90

ALTITUDE = 10,000 ft.



RANDOMDEC SIGNATURE

FILTER: 15.5 - 17.5 Hz

F = 16.7 Hz

$$2\zeta = g = \frac{1}{n\pi} \ln \left(\frac{X_0}{X_n} \right) = .095$$

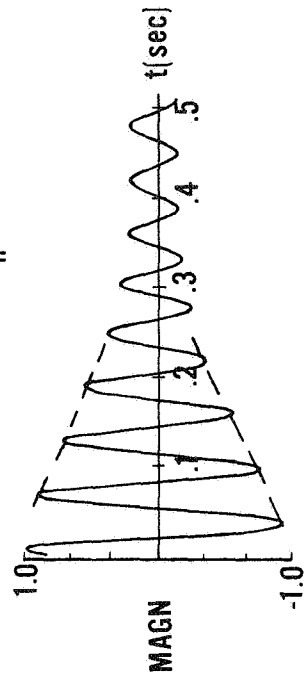


Figure 13.- AFFTC flutter test results:
random noise excitation.
(10,000 ft = 3048 m)